

# Hybrid Action Based Reinforcement Learning for Multi-Objective Compatible Autonomous Driving

Guizhe Jin, Zhuoren Li, Bo Leng, Wei Han, Lu Xiong, and Chen Sun

**Abstract**—Reinforcement Learning (RL) has shown excellent performance in solving decision-making and control problems of autonomous driving, which is increasingly applied in diverse driving scenarios. However, driving is a multi-attribute problem, leading to challenges in achieving multi-objective compatibility for current RL methods, especially in both policy execution and policy iteration. On the one hand, the common action space structure with single action type limits driving flexibility or results in large behavior fluctuations during policy execution. On the other hand, the multi-attribute weighted single reward function result in the agent’s disproportionate attention to certain objectives during policy iterations. To this end, we propose a Multi-objective Ensemble-Critic reinforcement learning method with Hybrid Parametrized Action for multi-objective compatible autonomous driving. Specifically, a parameterized action space is constructed to generate hybrid driving actions, combining both abstract guidance and concrete control commands. A multi-objective critics architecture is constructed considering multiple attribute rewards, to ensure simultaneously focusing on different driving objectives. Additionally, uncertainty-based exploration strategy is introduced to help the agent faster approach viable driving policy. The experimental results in both the simulated traffic environment and the HighD dataset demonstrate that our method can achieve multi-objective compatible autonomous driving in terms of driving efficiency, action consistency, and safety. It enhances the general performance of the driving while significantly increasing training efficiency.

**Index Terms**—Reinforcement learning, autonomous driving, motion planning, hybrid action.

## I. INTRODUCTION

Reinforcement learning (RL) has good potential in solving temporal decision-making problems [1], which can learn viable and near-optimal policies for complex tasks [2]. The RL agent explores policies through interactions with the environment, enabling self-improvement [3], [4]. Therefore, RL is considered as an effective way to solve decision-making and control problems for autonomous driving (AD) [5]. It has led to widespread application in driving scenarios [6] and has outperformed human drivers in certain tasks [7].

However, current RL methods still have several limitations in terms of compatibility with objectives such as driving efficiency, action consistency, and safety [8]. This does not satisfy the needs of multi-attribute driving tasks [9]. There

are two main reasons: i) The connection between action space structure and actual driving behavior during policy execution is overlooked; ii) With a large state space and multiple attributes strongly coupled in open driving environments, the agent has difficulty achieving efficient policy iteration while being multi-objective compatible. These two reasons cause limitations in policy performance.

For policy execution, directly utilizing a single-type action space to generate abstract or concrete driving behavior makes it challenging for the RL agent to both maintain flexibility and reduce driving behavior fluctuations. Specifically, a common approach involves having the agent generate discrete abstract driving goals, such as semantic decisions [10] or target points that guide path planning [11]. However, since the agent does not directly control the vehicle’s movement, its ability to influence driving flexibility is limited. Recently, it has become a popular approach for agent to directly output concrete control commands [12]. However, these commands, generated directly by the network, are prone to frequent fluctuations and abrupt responses to dynamic environmental changes.

In terms of policy iteration, it is mainly carried out through policy evaluation and policy exploration. For evaluation, a single reward function may not be compatible with all driving objectives, potentially causing the policy converge to local optimal. Specifically, when multiple attributes of an AD task are weighted into a single reward function, the agent may allocate disproportionate attention to certain attributes during training [8]. In an attempt to maximize rewards in certain states, some attributes may be neglected, leading to an inaccurate estimation of the value of those states. This may result in the driving performance being incompatible with the expectation of multiple objectives, such as becoming overly aggressive to maximize speed or excessively conservative to ensure safety. For exploration, performing random policy exploration based only on evaluated values lacks the orientation, causing the agent unable to actively explore unknown regions to discover potentially viable policies [13]. This random mechanism will lead agent to collect numerous repetitive exploration experiences that contribute little to the policy iterative update, resulting in inefficient policy convergence.

To address the above issues, this paper proposes an Multi-objective Ensemble-Critic reinforcement learning method with Hybrid Parametrized Action space (HPA-MoEC) for multi-objective compatible autonomous driving. Our hybrid parametrized action space includes a discrete action set and corresponding continuous parameters, which generate driving actions that combine both the abstract guidance and concrete control commands. Building on this, we define multiple reward

Guizhe Jin, Zhuoren Li, Bo Leng, Wei Han and Lu Xiong are with the School of Automotive Studies, Tongji University, Shanghai 201804, China. (Email: jgz13573016892@163.com, 1911055@tongji.edu.cn, lengbo@tongji.edu.cn, tjhanwei@foxmail.com, xiong\_lu@tongji.edu.cn).

Chen Sun is with the Department of Data and Systems Engineering, University of Hong Kong, Hong Kong. (Email: c87sun@hku.hk).

This work has been submitted to the IEEE for possible publication. Copyright may be transferred without notice, after which this version may no longer be accessible.

functions to decouple the attributes, with each reward function guiding one critic (i.e., value network) to focus on different objectives, cooperatively helping the actor (i.e., policy network) learn multi-objective compatible policies. Meanwhile, we introduce uncertainty to guide the agent in exploring viable driving policies, enabling more efficient exploration in unknown environments. The main contributions of our method are summarized as follows:

- 1) A hybrid parameterized action-based RL framework is proposed, which combines finer-grained guidance and control commands. The hybrid action space has consistently optimal discrete actions and their corresponding continuous action parameters. They further together generate abstract guidance and concrete control command outputs. Our method effectively achieves higher driving flexibility and smaller behavior fluctuations, ensuring the compatible in driving efficiency and action consistency.
- 2) A multi-objective compatible policy evaluation module is established, where critics focus on different objectives based on distinct reward functions. Given the safety-critical nature of AD, we set two driving objectives and evaluate them with two critics to verify the effectiveness of our design. One focuses on general performance, including interactivity, and the other on safety. Our design promotes multi-objective compatibility, with improvements in both general performance and safety demonstrated in the experimental results.
- 3) An epistemic uncertainty-based exploration strategy is designed for hybrid action, employing an ensemble of critics. By dynamically adjusting the direction and extent of exploration based on uncertainty and its changing trends, the agent is encouraged to faster explore regions of higher uncertainty for potentially viable policies. Our exploration strategy improves the learning efficiency of viable multi-objective compatible policies.

The remainder of this paper is organized as follows: Section II reviews related work, while Section III outlines the methodology. Specific implementation details are presented in Section IV. Section V discusses the experimental results, and the conclusions are provided in Section VI.

## II. RELATED WORKS

The AD task involves making complex sequential decisions in a dynamic environment and can therefore be modeled as Markov Decision Processes (MDPs) [14]. The MDP is commonly represented as a tuple  $\langle \mathcal{S}, \mathcal{A}, \mathcal{R}, \mathcal{T}, \gamma \rangle$ , where  $\mathcal{S}$  is the state space,  $\mathcal{A}$  is the action space,  $\mathcal{R}$  is the reward function,  $\mathcal{T}$  is the transition function, and  $\gamma$  is the discount factor. At time  $t$ , the RL agent selects action  $a_t \in \mathcal{A}$  based on state  $s_t \in \mathcal{S}$ , then receives reward  $r_t \in \mathcal{R}$  from the environment and transitions to state  $s_{t+1}$  according to  $\mathcal{T}$ . The goal of the agent is to find an optimal policy through trial-and-error to maximize the expected reward. Next, we will introduce three aspects of related work on our method:

### A. Action Space Structure

Many current RL methods use a single action type to control vehicle driving, which fail to be compatible with

high flexibility and small behavior fluctuations. On one hand, some studies use a discrete action space to generate abstract behavior decisions, offering long-term targets that indirectly guide vehicle control. Specifically, [15], [16] use DQN and its improved versions to generate semantic lateral actions, such as left or right lane changes. Additionally, [17], [18] introduces longitudinal discrete acceleration and deceleration actions. To provide clearer guidance, some studies select from a discrete set of trajectories [19], [20] or directly generate the positions and desired speeds of target points [21]. However, these methods often reduce the alignment between agent outputs and driving behavior, as they rely on integration with a basic controller for vehicle control, which limits flexibility. On the other hand, some studies [22], [23] directly generate steering angles laterally and accelerations longitudinally from a continuous action space, aiming to enhance flexibility. However, fluctuations in the network's output can cause frequent changes in steering angle and acceleration commands [24]. In scenarios with dedicated lanes, lateral fluctuations caused by steering angle variations will result in unpredictable paths. The experimental results in [12] provide further evidence for the existence of driving behavior fluctuations. In contrast, fluctuations in longitudinal acceleration are manageable and enable more flexible speed trajectories [25].

For compatibility of flexibility and small behavior fluctuations, several studies design hybrid actions by discretizing parts of a continuous action space [26], [27], or using a parameterized action space [12], [25], [28], which generates both lateral discrete abstract targets and longitudinal continuous concrete acceleration commands. Additionally, [29] designs a dual-layer decision-making control model that combines parallel DQN and DDPG for hybrid output. [30] trains skill-agents for various driving objectives to output acceleration, from which DQN can flexibly select. However, the hybrid action methods mentioned above only generate discrete abstract targets, while our work further focuses on providing finer-grained abstract guidance for steering angle.

### B. Multi-Objective Policy Evaluation

For AD problems, multiple attitudes should be considered, requiring the policy to be multi-objective compatible. The objectives are sometimes conflicting, like safety and driving efficiency [6]. The most common design is to linearly combine all attributes into a single, additive reward function for policy evaluation [31]. Specifically, the weights of this linearly expressed reward function are typically determined through manual design after multiple trial-and-error iterations [32], or by applying Inverse-RL to human demonstrations [33]. However, policy evaluation under this linear assumption may be inaccurate because the highest rewarding action may not be the one that enables multi-objective compatible driving, leading to reduced policy performance [34]. Additionally, a single critic representing multiple attitude rewards forces the learning of value coherence, which may not accurately reflect the true critic and degrade policy quality [35].

Some recent studies aim to develop architectures with multiple critics for multi-objective policy evaluation. In particular,

they use several reward functions to separate key attributes from a single reward function, treating each attribute as an independent evaluation objective, such as safety [36], driving efficiency [37], and comfort [38]. Additionally, [39] introduces a pre-trained safe-critic to guide the policy towards safer actions. However, further investigation is required within a hybrid action-based RL framework.

### C. Policy Exploration Strategy

Policy exploration helps agents discover potentially multi-objective compatible policies. A proper policy exploration strategy can significantly accelerate the learning process to converge to a viable policy faster [40]. However, the most common exploration strategy in RL is random exploration, such as  $\epsilon$ -greedy [41], which decreases exploration as training progresses. This randomized mechanism makes policy exploration lack of orientation and leads to repeated collection of experience samples, which reduces the training efficiency. Although some studies attempt to introduce noisy [42], reward novel state [43] or error of reward [44] to modify the exploration level, this does not change the nature of random exploration. Some other studies [45] attempt to use reward shaping to encourage exploration, but the manually imposed rewards heavily depend on the designer's experience.

Some studies [46], [47] use model ensemble technique to capture epistemic uncertainty and select actions that encourage the agent to explore high-uncertainty areas, thus accelerating policy training. Few studies leverage epistemic uncertainty in AD tasks to improve driving policy training efficiency [48]. In addition, most current methods only explore policies for a single action type.

## III. METHODOLOGY

In this section, we will present the overall framework and specific formulation details related to the HPA-MoEC methodology.

### A. Overall Framework

The method proposed in this paper is based on a hybrid parameterized action space for policy evaluation and improvement, considering multiple objectives to achieve multi-objective compatibility. Thus, the MDP can be rewritten as a new tuple  $\langle \mathcal{S}, \mathcal{H}, [\mathcal{R}_1, \dots, \mathcal{R}_N], \mathcal{T}, \gamma \rangle$ , where:

- $\mathcal{H}$  represents the hybrid parameterized action space, where  $\mathcal{H} = \{(o, a_o) | a_o \in \mathcal{A}_O, \text{ for } \forall o \in \mathcal{O}\}$ . The  $o$  is the discrete action option selected from the discrete action option set  $\mathcal{O}$ . The  $a_o$  can be seen as the continuous action parameter corresponding to  $o$ , drawn from the continuous interval  $\mathcal{A}_O$  corresponding to  $\mathcal{O}$ .
- $[\mathcal{R}_1, \dots, \mathcal{R}_N]$  represents a set of  $N$  reward functions, where  $\mathcal{R}_i$  denotes the  $i$ -th reward function for  $i \in [1, \dots, N]$ .

As mentioned previously, AD tasks on structured roads require finer-grained abstract guidance to generate concrete control commands that reduce fluctuations while keeping flexibility in driving behavior. We design a hybrid action space

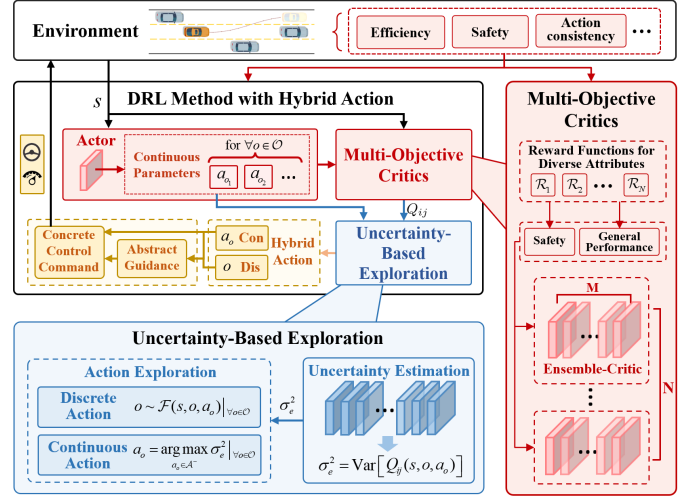


Fig. 1. The overall framework of proposed HPA-MoEC. The actor of RL Method firstly generates the continuous action parameters  $a_o$  based on states  $s$ , which are then input into the Multi-Objective Critics module along with  $s$  for evaluating the value function. This module consists of  $N$  ensemble-critics corresponding to the different attributes, and each of them is an ensemble of  $M$  critics. The Exploration Strategy module then captures epistemic uncertainty from the ensemble-critics and selects the final hybrid action  $(o, a_o)$  that enhances training efficiency.

that enables the agent to simultaneously output discrete actions  $o$  and continuous action parameters  $a_o$ , ensuring optimality in both. These outputs are then used to generate both abstract guidance and concrete control commands. Specifically, lateral concrete control commands are generated by combining abstract guidance with prior knowledge, while longitudinal commands are directly derived from  $a_o$ .

In addition, the agent should consider multiple attributes of the AD task during policy evaluation and efficiently explore multi-objective compatible viable policies. Therefore, we design the Multi-objective Ensemble-Critic framework, which takes  $N$  attributes as evaluation objectives and helps agent explore in high-certainty regions. Specifically, the framework consists of  $N$  ensemble-critics, which work together for policy evaluation based on the reward functions  $[\mathcal{R}_1, \dots, \mathcal{R}_N]$ , each focusing on different attributes. Meanwhile, each ensemble-critic consists of  $M$  critics. The epistemic uncertainty  $\sigma_e$  and its change trend can be captured through ensemble-critic, which helps to orient exploration. The overall framework of the proposed HPA-MoEC method is shown in Fig. 1.

### B. Policy and Value Function Representation

Under the hybrid parameterized action space, the state-action value function of the optimal policy can be described by the Bellman optimal equation as follows:

$$Q(s_t, o_t, a_{o,t}) = \mathbb{E} \left[ r_t + \gamma \max_{o \in \mathcal{O}} \left\{ \sup_{a_o \in \mathcal{A}_O} Q^i(s_{t+1}, o, a_o) \right\} \right]. \quad (1)$$

HPA-MoEC consists of  $N$  ensemble-critics, each composed of  $M$  critics, resulting in a total of  $N \times M$  critics for value function evaluation. Specifically, each critic can estimate the value of the action  $(o, a_o)$  in state  $s$  based on its focused attributes.

Let  $Q_{ij}$  represents the optimal value function evaluated by the  $i$ -th critic corresponding to  $\mathcal{R}_i$ :

$$Q_{ij}(s_t, o_t, a_{o,t}) = \mathbb{E} \left[ r_t^i + \gamma \max_{o \in \mathcal{O}} \left\{ \sup_{a_o \in \mathcal{A}_O} Q_{ij}(s_{t+1}, o, a_o) \right\} \right] \quad (2)$$

where  $j \in [1, \dots, M]$ ,  $r_t^i = \mathcal{R}_i(s, o, a_o)$ . However, finding the optimal continuous action  $a_o$  is challenging in a hybrid parameterized action space. To overcome this, we assume that the value function is fixed, meaning that for any state  $s$  and discrete action  $o$ , the  $a_o$  depends on state  $s$ . At this stage, the problem of optimizing in the continuous space becomes determining the mapping from state  $s$  to action  $a_o$ :  $\mathcal{S} \rightarrow \mathcal{A}_O$ . By using a deterministic policy network  $\mu(s; \theta^\mu)$  to approximate this mapping, the continuous action  $a_o$  can be obtained, with network parameters  $\theta_\mu$ . This policy network is known as the actor. Meanwhile, a value network is employed to approximate the value function  $Q_{ij}$ , with parameters  $\theta_{ij}^Q$ . Given the assumption that the value function is fixed, the MDP in the parameterized action space can be viewed as the process of exploring  $\theta^\mu$  for a given  $\theta_{ij}^Q$ :

$$Q_{ij}(s, o, \mu(s; \theta^\mu); \theta_{ij}^Q) \approx \sup_{a_o \in \mathcal{A}_O} Q_{ij}(s, o, a_o; \theta_{ij}^Q) |_{\forall o \in \mathcal{O}}. \quad (3)$$

Specifically, this process can be approximated using a two-timescale update rule [49], where the training update step size for  $\theta_{ij}^Q$  is much larger than that for  $\theta_{ij}^\mu$ . Therefore,  $Q_{ij}$  can be expressed as:

$$Q_{ij}(s_t, o_t, a_{o,t}; \theta_{ij}^Q) = \mathbb{E} \left[ r_t^i + \gamma \max_{o \in \mathcal{O}} Q_{ij}(s_{t+1}, o, \mu(s_{t+1}; \theta^\mu); \theta_{ij}^Q) \right]. \quad (4)$$

The fundamental target for updating a single critic is:

$$y_{ij,t} = r_t^i + \gamma \max_{o \in \mathcal{O}} Q'_{ij}(s_{t+1}, o, \mu'(s_{t+1}; \theta^{\mu'}); \theta_{ij}^{Q'}) \quad (5)$$

where,  $Q_{ij}'$  and  $\mu'$  are the target networks used to assist in updating the critic and actor, with parameters  $\theta_{ij}^{Q'}$  and  $\theta_{ij}^{\mu'}$ , respectively.

In our multi-objective policy evaluation architecture, each critic is not updated independently. For each ensemble-critic, every critic within shares the same driving attribute. Then, all ensemble-critics collaborate to guide the actor in learning a multi-objective compatible driving policy. To ensure consistency among all critics in evaluating driving behavior, the evaluation results—both for specific attributes and overall performance—should be fed back to each critic, for updating networks. Therefore, it is necessary to construct the critic's update target from both the ensemble-critic perspective and the multi-objective compatible overall perspective. For the  $i$ -th ensemble-critic, its overall evaluation of the policy's

performance under a given attribute is the expectation of the value provided by the  $M$  critics:

$$\begin{aligned} \bar{Q}_i(s_t, o, a_{o,t}) &= \mathbb{E}_{j \in [1, \dots, M]} \left[ Q_{ij}(s_t, o, \mu(s_{t+1}; \theta^\mu); \theta_{ij}^Q) \right] \\ &= \frac{1}{M} \sum_{j=1}^M Q_{ij}(s_t, o, \mu(s_{t+1}; \theta^\mu); \theta_{ij}^Q) |_{\forall o \in \mathcal{O}}. \end{aligned} \quad (6)$$

Correspondingly, the overall target of this ensemble-critic during training can be expressed as:

$$\bar{y}_{i,t} = r_t^i + \gamma \max_{o \in \mathcal{O}} \bar{Q}'_i(s_{t+1}, o, a_{o,t+1}), \quad (7)$$

where  $\bar{Q}'_i$  is the expectation of all  $Q'_{ij}$  for  $j \in [1, \dots, M]$ , similar to Eq.(6).

In addition, the actor's outputs assign different attention to the  $N$  ensemble-critics, according to the weights  $\omega_i$ . Thus, the value function for evaluating the policy's multi-objective compatibility at the overall level can be represented as follows:

$$Q_{all}(s_t, o, a_{o,t}) = \sum_{i=1}^N \omega_i \bar{Q}_i(s_t, o, a_{o,t}) |_{\forall o \in \mathcal{O}}, \quad (8)$$

where  $\sum_i \omega_i = 1$ . Building on this, the overall target for all critics in the HPA-MoEC can be written as:

$$y_{all,t} = r_t^{all} + \gamma \max_{o \in \mathcal{O}} Q'_{all}(s_{t+1}, o, a_{o,t+1}), \quad (9)$$

where  $r^{all}$  combines the attribute rewards based on the attention level of each ensemble-critic, i.e.,  $r^{all} = \sum_i \omega_i r^i$ . The  $Q'_{all}$  is represented by the weighted sum of  $Q'_i$ , similar to Eq.(8).

Thus, the update of the  $\theta_{ij}^Q$  considers not only the critic's own TD error but also the average TD error of all critics in the ensemble for a given attribute, and the overall TD error of all critics. For these three aspects, corresponding loss functions are defined as follows:

$$\mathcal{L}_{ij,t}(\theta_{ij}^Q) = \frac{1}{2} [y_{ij,t} - Q_{ij}(s_t, o_t, a_{o,t}; \theta_{ij}^Q)]^2, \quad (10)$$

$$\mathcal{L}_{i,t}(\theta_{ij}^Q) = \frac{1}{2} [y_{i,t} - \bar{Q}_i(s_t, o_t, a_{o,t})]^2, \quad (11)$$

$$\mathcal{L}_{all,t}(\theta_{ij}^Q) = \frac{1}{2} [y_{all,t} - Q_{all}(s_t, o_t, a_{o,t})]^2. \quad (12)$$

To prevent any critic from significantly deviating due to random factors and disrupting policy convergence, we have added a guiding term to the loss function of the parameter  $\theta_{ij}^Q$ . This helps ensure that all critics in the ensemble-critic are updated in a similar direction:

$$\mathcal{L}_{conv,t}(\theta_{ij}^Q) = \frac{1}{2} [Q_{ij}(s_t, o_t, a_{o,t}; \theta_{ij}^Q) - \bar{Q}_i(s_t, o_t, a_{o,t})]^2. \quad (13)$$

In summary, when updating the parameters  $\theta_{ij}^Q$ , the final loss function account for the four aspects discussed earlier:

$$\mathcal{L}_t(\theta_{ij}^Q) = \lambda_t \cdot \mathbf{L}_t^T. \quad (14)$$

where  $\mathbf{L}_t = [\mathcal{L}_{ij,t}, \mathcal{L}_{i,t}, \mathcal{L}_{all,t}, \mathcal{L}_{conv,t}]$  represents the vector of loss function and  $\lambda_t = [\lambda_1, \lambda_2, \lambda_3, \lambda_4]$  is the corresponding weight vector.

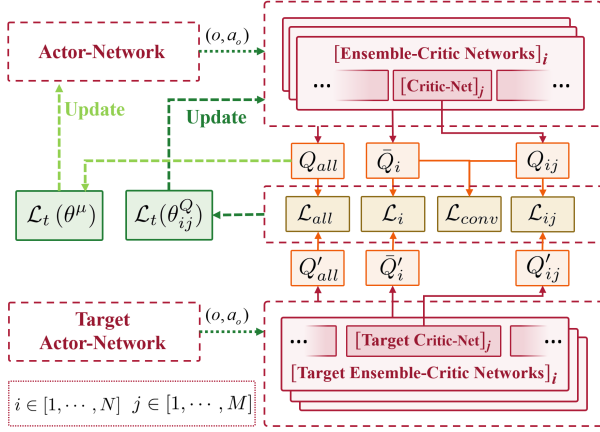


Fig. 2. The network parameter update process for actor and any critic. The target networks are soft-updated.

The target for updating the actor is more straightforward, i.e., finding a multi-objective compatible optimal policy by maximizing the overall value function:

$$\mathcal{L}_t(\theta^\mu) = -\frac{1}{M} \sum_{i=1}^N \omega_i \sum_{j=1}^M \sum_{o \in \mathcal{O}} Q_{ij}(s_t, o, \mu(s_{t+1}; \theta^\mu); \theta_{ij}^Q). \quad (15)$$

Overall, the updating process of the actor's parameter  $\theta^\mu$  and any critic's parameter  $\theta_{ij}^Q$  is shown in Fig. 2.

### C. Uncertainty Estimation and Exploration Strategy

Epistemic uncertainty reflects the agent's lack of knowledge due to incomplete learning and can be captured by ensemble-critic [50]. In the  $i$ -th ensemble-critic, a larger discrepancy between the evaluation results of the critics indicates higher epistemic uncertainty about the corresponding attribute. Such discrepancies can be quantified by the variance, so the epistemic uncertainty  $\sigma_{e,i}^2$  of the  $i$ -th attribute is:

$$\sigma_{e,i}^2(s, o, a_o) = \text{Var}_{j \in [1, \dots, M]} [Q_{ij}(s, o, a_o)] |_{\forall o \in \mathcal{O}}. \quad (16)$$

Considering that different attention levels are assigned to each ensemble-critic to achieve multi-objective compatibility, the weights  $\omega_i$  are also used to compute the agent's total epistemic uncertainty:

$$\sigma_e^2(s, o, a_o) = \sum_{i=1}^N \omega_i \sigma_{e,i}^2(s, o, a_o) |_{\forall o \in \mathcal{O}}. \quad (17)$$

In the parameterized action space,  $a_o$  is treated as a parameter of  $o$ . Thus, the change in epistemic uncertainty for any action pair  $(o, a_o)$  can be captured by the gradient:

$$\mathcal{G} = \nabla_{a_o} \sigma_e^2(s, o, a_o) |_{\forall a_o \sim \mu(s)}. \quad (18)$$

Additionally, it is necessary to clarify that  $\sigma_e^2(s, o, a_o)$  represents the epistemic uncertainty of the state-action pair for  $\forall o \in \mathcal{O}$ , while the overall uncertainty of the environment at state  $s$  is denoted as  $\sigma_e^2(s)$ . Specifically, the two are related as follows:

$$\sigma_e^2(s) = \mathbb{E} [\sigma_e^2(s, o, a_o)] |_{\forall o \in \mathcal{O}} = \frac{1}{|\mathcal{O}|} \sum_{o \in \mathcal{O}} \sigma_e^2(s, o, a_o). \quad (19)$$

Oriented by the captured epistemic uncertainty, the agent employs two different exploration strategies for the discrete action  $o$  and its corresponding continuous action  $a_o$  while exploring potentially viable policies. For continuous action, the agent's final executed  $a_o$  is determined by both the actor's output and the chosen  $o$ . Thus, the ideal continuous action exploration strategy is to solve a nonlinear continuous optimization problem:  $\arg \max_{a_o \in \mathcal{A}_\mathcal{O}} \sigma_e^2(s, o, a_o) |_{\forall o \in \mathcal{O}}$ , to maximize exploration across all discrete actions  $o$ . However, solving this problem is computationally expensive and impractical for efficient policy training. Therefore, we choose a cheaper alternative by constructing a finite set of actions  $\mathcal{A}^-$ , where  $\mathcal{A}^- \subset \mathcal{A}_\mathcal{O}$ , based on the actor's origin output and epistemic uncertainty gradient. This discretizes the problem of selecting high-uncertainty actions in the continuous domain:

$$\mathcal{A}^- = \left\{ a_o \mid a_o = \text{sat}_{\mathcal{A}_\mathcal{O}} \left[ \mu(s) + \frac{k \cdot \varsigma}{K} \mathcal{G} \right], k \sim \mathcal{U}(1, K) \right\}, \quad (20)$$

$$a_o = \arg \max_{a_o \in \mathcal{A}^-} \sigma_e^2(s, o, a_o) |_{\forall o \in \mathcal{O}}, \quad (21)$$

where  $\mathcal{U}(1, K)$  denotes a uniform distribution over integers from 1 to  $K$ . The  $\varsigma$  is a coefficient that decreases with training steps, where  $\varsigma \in (0, 1)$ , reflecting the agent's focus on exploring actions. This simplified approach enhances continuous action exploration with low computational cost.

Similarly, the most exploratory discrete action is the one that maximizes epistemic uncertainty:  $\arg \max_{o \in \mathcal{O}} \sigma_e^2(s, o, a_o)$ . However, when the epistemic uncertainty of all discrete actions in the set  $\mathcal{O}$  is low, relying on epistemic uncertainty to choose actions contributes little to strategy exploration, since the agent is already confident about all actions. Thus, we define an uncertainty threshold  $\sigma_{e,th}^2$  to ensure the agent adopts a greedy strategy and maximizes reward when its uncertainty is low. Additionally, since the parameters of the critic-networks are randomly initialized and their outputs may fluctuate, the estimation of epistemic uncertainty has fluctuations. We use a probabilistic approach rather than directly selecting the action with maximum uncertainty. Specifically, similar to the *Softmax* function, the probability of selecting a discrete action is based on its uncertainty value, with the total probability across all actions summing to 1. Therefore, the selection of discrete actions follows the function  $\mathcal{F}$ , where  $o \sim \mathcal{F}(s, o, a_o) |_{\forall o \in \mathcal{O}}$ :

$$\mathcal{F} = \begin{cases} o \sim \varepsilon(s, o, a_o) |_{\forall o \in \mathcal{O}} & \text{if } \varsigma \sigma_e^2(s) > \sigma_{e,th}^2 \\ \arg \max_{o \in \mathcal{O}} Q_{all}(s, o, a_o) & \text{else} \end{cases}, \quad (22)$$

$$\varepsilon(s, o, a_o) = \frac{e^{\sigma_e^2(s, o, a_o)}}{\sum_{o \in \mathcal{O}} e^{\sigma_e^2(s, o, a_o)}} |_{\forall o \in \mathcal{O}}, \quad (23)$$

where  $\varepsilon$  indicates the probability of choosing each action.

Based on the methods discussed above, we provide the complete algorithmic training process for our HPA-MoEC in Algorithm 1.

## IV. IMPLEMENTATION

This section presents the implementation details of using HPA-MoEC to perform the AD lane-changing task, including MDP formulation, training setup, and comparison models.

---

**Algorithm 1** Training process of proposed HPA-MoEC
 

---

**Require:** Step sizes  $\{\alpha, \beta\}$ , total training steps  $T$ , soft-update parameter  $\tau$ , number of critics in ensemble-critic  $M$ , attribute weight  $\omega$ , loss function weight  $\lambda$ .

- 1: **Initialize:** networks  $\{\{Q_{ij}\}, \mu, \{Q'_{ij}\}, \mu'\}$  with random parameters  $\{\{\theta_{ij}^Q\}, \theta^\mu, \{\theta_{ij}^{Q'}\}, \theta^{\mu'}\}$  for  $i \in [1, \dots, N]$  and  $j \in [1, \dots, M]$ , replay buffer size  $D$ , exploration parameter  $\varsigma$ .
- 2: **for**  $t = 0$  to  $T$  **do**
- 3:   Get state  $s_t$  from environment.
- 4:   Capture  $\sigma_e^2$  and its gradient according to Eq. (16) (18).
- 5:   Select  $a_{o,t}$  for  $\forall o \in \mathcal{O}$ , according to Eq. (21).
- 6:   Select  $o_t$  according to Eq. (22).
- 7:   Generate abstract guidance by  $o_t$  and  $a_{o,t}$ .
- 8:   Generate concrete control commands for EV.
- 9:   Get  $s_{t+1}$  and  $r_t^i$  from environment, for  $i \in [1, \dots, N]$ .
- 10:   Store  $\{s_t, (o_t, a_{o,t}), [r_t^1, \dots, r_t^N], s_{t+1}\}$  into  $D$ .
- 11:   Sample transitions randomly from  $D$ .
- 12:   Compute  $\mathcal{L}_t(\theta_{ij}^Q), \mathcal{L}_t(\theta^\mu)$ , according to Eq. (14)(15).
- 13:   Update  $\theta_{ij,t+1}^Q \leftarrow \theta_{ij,t}^Q - \alpha_t \nabla \mathcal{L}_t(\theta_{ij}^Q)$ .
- 14:   Update  $\theta_{ij,t+1}^\mu \leftarrow \theta_{ij,t}^\mu - \beta_t \nabla \mathcal{L}_t(\theta^\mu)$ .
- 15:    $\theta_{ij,t+1}^{Q'} \leftarrow \tau \theta_{ij,t}^{Q'} + (1-\tau) \theta_{ij,t}^{Q'}$ ,  $\theta_{t+1}^{\mu'} \leftarrow \tau \theta_t^{\mu'} + (1-\tau) \theta_t^{\mu'}$ .
- 16:   update  $\varsigma, s_t \leftarrow s_{t+1}$ .
- 17:   **if**  $s_t$  is terminal **then**
- 18:     Reset environment.
- 19:   **end if**
- 20: **end for**
- 21: **return**

---

### A. MDP Formulation

1) *State Space:* For the agent to learn a driving policy that can handle the lane-changing task, the state space design must include all relevant factors that could impact lane-changing behavior. Specifically, the state space includes feature information about the Ego Vehicle (EV) and six surrounding vehicles (SVs) in its current and adjacent lanes:

$$\mathcal{S} \triangleq \left\{ \begin{array}{c} [ID_{lane}, x, y, \varphi, v_x, v_y]^{\text{EV}}, \\ [p_n, \Delta x_n, \Delta y_n, \varphi_n, \Delta v_{x,n}, \Delta v_{y,n}]_{n \in [1 \dots 6]}^{\text{SVs}} \end{array} \right\}, \quad (24)$$

where the state of the EV in the road coordinate system consists of six variables: lane ID, longitudinal and lateral position, heading angle, and longitudinal and lateral velocity. For the  $n$ -th SV, the relevant information includes: a presence flag, longitudinal and lateral position relative to the EV, heading angle, and longitudinal and lateral velocity relative to the EV. Notably, the EV only monitors SVs within the longitudinal observation range  $\Delta x \in [-80m, 160m]$ .

2) *Hybrid Parameterized Action Space:* For the lane-changing task, we design explicit hybrid parameterized actions as follows: i) discrete semantic decision action  $b$ , ii) continuous parameter  $l$  for constructing a guiding path, and iii) continuous acceleration command  $acc$ . The concrete correspondence is:  $b \leftarrow o, (l, acc) \leftarrow a_o$ . Specifically,  $b$  is selected from a discrete set  $\{LLC : -w_r, RLC : w_r, LK : 0\}$ , where  $w_r$  represents the road width, with  $LLC$  and  $RLC$  representing left and right lane-change, respectively, and  $LK$  indicating lane-keeping.

Considering the vehicle kinematic model [31], the value range for  $l$  is defined as follows:

$$l \in \left[ \min \left( \sqrt{4R_0 w_r - w_r^2}, \frac{v_x^2}{2acc_{\max}^-} \right), e^{|v_x| + w_r} \right], \quad (25)$$

where  $R_0$  and  $acc_{\max}^-$  represent the minimum turning radius and maximum braking acceleration of the EV. In addition, the range of the acceleration command  $acc$  is  $[-3m/s^2, 3m/s^2]$ .

At each time step  $t$ , with  $(b_t, l_t, acc_t)$  output by the agent, the positions of the guiding path points can be generated using a polynomial curve-based formula:

$$y_{0,t+k} = \sum_{m=0}^5 \gamma_m x_{0,t+h}^m, \quad \text{where } h \in [1, \dots, H_p], \quad (26)$$

where  $(x_{t+h}, y_{t+h})$  represents the position of the point at time step  $t+h$ , and  $H_p$  is the planning horizon. The coefficients  $\gamma_m$  of the polynomial curve can be obtained by solving a system of linear equations. Specifically, the EV's position and heading at the starting point are known, while the heading at the end point can be obtained from the road information [6]. Actually, the guiding path is determined by the selection of its endpoint position  $(x_{t+H_p}, y_{t+H_p})$ , which is derived from the RL agent's output, where  $x_{t+H_p} = l_t$  and  $y_{t+H_p} = b_t$ . As the guiding path generated, the EV's steering angle command  $\delta$  is output using prior knowledge, specifically the Stanley algorithm in this paper. Finally, both the steering angle  $\delta$  and the acceleration  $acc$  are used together for EV driving control.

3) *Reward Function for Multi-Objective:* Since safety is the fundamental requirement for driving, safety attribute is treated as a distinct objective and a corresponding safety reward function is designed for one ensemble-critic. Other attributes are combined into a single general performance reward function for another ensemble-critic. This enhances the RL agent's compatibility with safety and general driving performance.

The safety reward function,  $\mathcal{R}_{safe}$ , focuses on safety in two aspects:

$$\mathcal{R}_{safe} = -10f_{unsafe} + 0.5\text{sat}_{[0,1]} \left[ \frac{\Delta t}{t_{\max}} \right], \quad (27)$$

where,  $f_{unsafe}$  is set to 1 when the EV goes off the road or collides with SVs, and 0 otherwise. To further identify potential safety risks, the safety reward function also includes the TTC (Time to Collision) metric, where  $\Delta t$  is the estimated time to collision between the EV and the vehicle ahead, and  $t_{\max}$  is the maximum time for TTC evaluation. The values 10 and 0.5 are the weights assigned to the two aspects mentioned above, respectively.

The general performance reward function,  $\mathcal{R}_{gen}$ , incorporates considerations of efficiency, comfort, and interaction:

$$\begin{aligned} \mathcal{R}_{gen} &= \mathcal{R}_{eff} + \mathcal{R}_{comf} + \mathcal{R}_{int} \\ \mathcal{R}_{eff} &= \frac{|v - v_t|}{v_t} - \max(0, \frac{v_p - v}{v_p}) \\ \mathcal{R}_{comf} &= -0.5 \frac{|\delta|}{|\delta_{\max}|} - 0.5 \frac{|acc|}{|acc_{\max}|} \\ \mathcal{R}_{int} &= -0.1 \sum_{n=1}^6 \frac{|acc_n^{SV}|}{|acc_{\max}|}, \end{aligned} \quad (28)$$

where  $\mathcal{R}_{eff}$  is efficiency reward, encouraging the EV to maintain a speed close to the target  $v_t$ . Meanwhile, a low-speed penalty is applied to minimize the impact of the vehicle's deceleration on overall traffic flow, with the threshold set at  $v_p$ . The  $\mathcal{R}_{comf}$  is comfort reward, related to the action consistency of steering angle and acceleration, where  $\delta_{max}$  and  $acc_{max}$  denote the maximum values of the two control commands. Moreover,  $\mathcal{R}_{int}$  represents the interaction reward, penalizing EV's interference with SV's motion while interacting with environment. The  $acc_n^{SV}$  denotes the observed acceleration of the  $n$ -th SV. The number before each item is the weight of the attention given to it.

### B. Training Setup

We developed a three-lane structured road environment using the AD simulation platform, highway-env [51], in which the EV attempts to accomplish a multi-objective compatible lane-changing driving task. Specifically, all vehicles, including the EV, are randomly placed on the three-lane road with random initial speeds. The IDM and MOBIL models are applied to control the longitudinal and lateral movements of the SVs [31]. The SVs may change lanes at appropriate times to get closer to the target speed, potentially disrupting the EV. Additionally, we use the vehicle capacity (V/C) to represent traffic congestion, setting it to 0.5 to create moderate congestion. This ensures the EV has enough space to change lanes without oversimplifying the environment.

During training, the episode ends when  $f_{unsafe} = 1$ , after which the environment and all vehicles are reinitialized. Each episode is capped at 200 seconds to avoid the EV operating for long periods in low-variability scenarios. Details of the hyperparameter settings used in the algorithm training are provided in Table I.

TABLE I  
HYPERPARAMETERS

Para.	Item	Value
$M$	Number of critics in an ensemble-critic	6
$\omega_1, \omega_2$	Weights of $\mathcal{R}_{safe}$ and $\mathcal{R}_{gen}$	0.4, 0.6
$\gamma$	Discount factor	0.9
$\alpha$	Training step size of critic	0.01
$\beta$	Training step size of actor	0.001
$\lambda$	Weights of loss functions for critic	[0.5, 0.2, 0.2, 0.1]
$K$	parameters for con-action exploration	10
$\tau$	Soft-update parameter	0.005
$T$	Number of steps for training	200000
$\varsigma$	Exploration weight parameter	$1 \rightarrow 0.001$
—	Number of hidden layers in critic/actor	3
—	Hidden layer size	256
—	Activation function	Tanh
—	Replay buffer size	40000
—	Sample batch size	256
—	Training optimizer	Adam

Additionally, our method is tested on 200 episodes in both the training environment and the HighD [52] real-world dataset. For testing on the HighD dataset, the trained agent controls the vehicles exhibiting lane-changing behavior, while the SVs follow their predefined trajectories.

### C. Comparison Models

1) *Comparison Baseline*: To comprehensively evaluate the proposed HPA-MoEC, we compare it with several widely used RL methods for the AD lane-changing task. To ensure fairness, all methods share the same training and testing environments, as well as the state space. The main difference is that, unlike HPA-MoEC, the other methods couple the attributes into a single reward function:  $\mathcal{R}_{base} = \omega_1 \mathcal{R}_{safe} + \omega_2 \mathcal{R}_{gen}$ . More importantly, the action spaces structure and policy exploration strategies in the following methods differ:

- **Deep Q-Network (DQN)** [53]: It only generates discrete semantic decisions and is paired with a PID controller to control the EV. The exploration strategy used is  $\epsilon$ -greedy.
- **SAC with Continuous actions (SAC-C)** [54]: It only outputs continuous control commands, which are lateral steering angle and longitudinal acceleration. Its exploration is enhanced through maximum entropy and the addition of Gaussian noise to the actions.
- **SAC with Hybrid actions (SAC-H)** [54]: SAC-H discretizes part of the continuous action space in SAC, producing outputs similar to HPA-MoEC.
- **PPO with Hybrid actions (PPO-H)** [55]: An on-policy actor-critic algorithm with action space similar to SAC-H.

2) *Ablation Model*: To further validate the effectiveness of the three key techniques used in HPA-MoEC: i) hybrid parameterized actions with finer-grained abstract guidance; ii) a multi-objective compatible policy evaluation architecture; and iii) epistemic uncertainty-based policy exploration, we design the following ablation baselines:

- **HPA-MoEC**: The method proposed in this paper includes all three technical components.
- **HPA-Mo**: By removing component iii from HPA-MoEC, policy exploration is no longer oriented by uncertainty. Policy evaluation for each objective is performed by a single critic only, rather than by an ensemble-critic.
- **HPA**: By further removing component ii, only one overall objective remains, with one corresponding critic for evaluating policies that considers multiple attributes.
- **HPA w/o GP**: By further removing component i, this baseline generates only coarse-grained discrete semantic decisions as abstract guidance, which are combined with the PID controller to output steering angles. It retains a hybrid action space that also provides continuous acceleration commands.

### D. Evaluation Metrics

To evaluate the driving performance of the proposed method across multiple objectives, we used several metrics for each episode:

- **Average Reward (AR)**: AR is the ratio of total reward to episode length, offering a comprehensive evaluation of the RL agent's performance.
- **Collision Rate (CR, %)**: Collisions result from hazardous driving behavior and can be used to evaluate the safety of the agent's driving policy.



- Average Speed (AS,  $\text{m/s}$ ): The EV's speed indicates the agent's ability to intelligently execute lane changes actions to enhance driving efficiency.
- Number of Lane-change (NL): NL partially reflects the EV's flexibility and can be analyzed alongside AS to explain the reasons for improved driving efficiency.
- Variance of Steering angle (VS,  $\text{rad}^2$ ) and Acceleration (VA,  $\text{m}^2/\text{s}^4$ ): VS and VA respectively indicate the vehicle's fluctuations in lateral and longitudinal behavior, reflecting the consistency of the driving policy's actions.

## V. RESULTS AND DISCUSSIONS

### A. Training Performance

The learning curves for general performance and safety during training are shown in Fig. 3, with each algorithm trained six times using different seeds. The total reward curve and corresponding variance distribution in Fig. 3(a) show that the our HPA-MoEC achieves higher rewards with smaller policy fluctuations. This indicates that, regardless of seed variations, its policy consistently converges to the best general performance. By comparison, the similar rewards achieved by SAC-H and PPO-H indicate that both of them perform worse than HPA-MoEC. Furthermore, without finer-grained guiding paths, the reward during SAC-C convergence is much lower, indicating poorer driving performance when both longitudinal and lateral direct control commands are output together. Using only semantic decision actions, the DQN receives the lowest reward, indicating that discrete actions alone are insufficient for complex driving tasks.

Additionally, once the minimum sample size required for training is gathered in the experience replay pool, the policy improvement speed of HPA-MoEC is significantly faster than that of all the baselines. This increase in training efficiency is attributed to the introduction of an epistemic uncertainty-based exploration strategy, which enables a oriented and faster exploration of potentially viable policies. Notably, since SAC-C directly controls the EV by outputting steering angle commands, it often veers off the road and ends the episode early, causing the reward curve to differ significantly from other methods.

As shown in Fig. 3(b), the change in CR for each method during training is illustrated, with the zoomed-in view of the converged curves highlighting that HPA-MoEC ultimately maintains a low CR. Thanks to the decoupling of the safety objective from the general performance objective within the multi-objective policy evaluation architecture, the agent places greater emphasis on safety. In contrast, SAC-H and PPO-H have slightly higher CRs, whereas DQN has the highest. Notably, although SAC-C performs poorly in total reward, it prioritizes the safety of the EV by maintaining a very low CR. This results from its conservative following behavior, which will be discussed in detail in Section V-B1.

### B. Testing Performance

1) *Testing with Rule-Based SVs*: The boxplots in Fig. 4 illustrate the distribution of four metrics in testing: average reward (Fig. 4(a)), average speed (Fig. 4(b)), and the variance

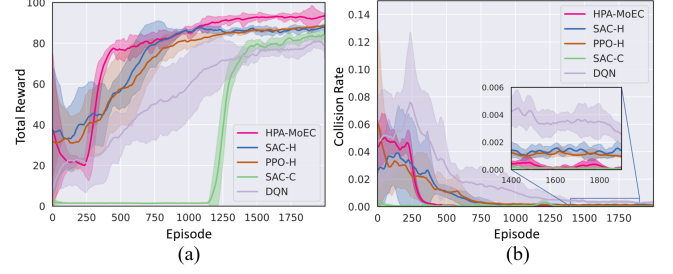


Fig. 3. The training process of our method with comparison methods quantified by: a) Total Reward and b) Collision Rate.

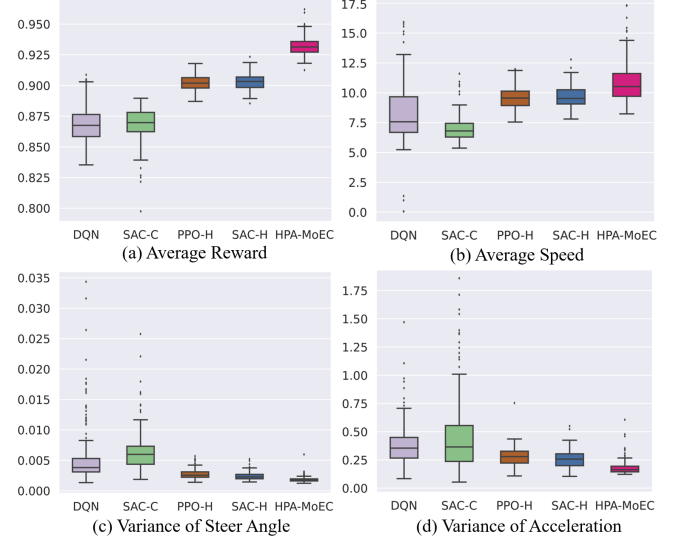


Fig. 4. Metrics distribution of testing with Rule-Based SVs: (a) average reward, (b) average speed, (c) variance of steering angle, (d) variance of acceleration.

TABLE II  
TEST RESULTS WITH RULE-BASED SVs

Method	AR	AS	NL	VS	VA	CR
DQN	0.860	8.18	7.71	0.0055	0.381	0.38%
SAC-C	0.868	6.95	2.04	0.0063	0.452	0.01%
PPO-H	0.902	9.57	5.76	0.0027	0.279	0.13%
SAC-H	0.903	9.62	5.57	0.0024	0.256	0.12%
HPA-MoEC	0.932	10.87	7.14	0.0019	0.181	0.04%

of steering angle and acceleration (Fig. 4(c) and Fig. 4(d)). The quantitative statistics for all metrics are provided in Table II. Specifically, the driving policy of the proposed HPA-MoEC demonstrates advantages in driving efficiency, action consistency, and safety.

In general, HPA-MoEC receives the highest AR, which is consistent with the training results and indicates a more effective driving policy. SAC-H and PPO-H also perform well, with similar AR levels. In contrast, the driving policy of DQN and SAC-C perform poorly and exhibit considerable fluctuation, with lower and more dispersed AR values.

**For driving efficiency**, HPA-MoEC achieves the highest AS through more flexible lane changes. In comparison, SAC-H and PPO-H have lower ASs due to reduced lane-changing flexibility, leading to suboptimal efficiency. Specifically, com-



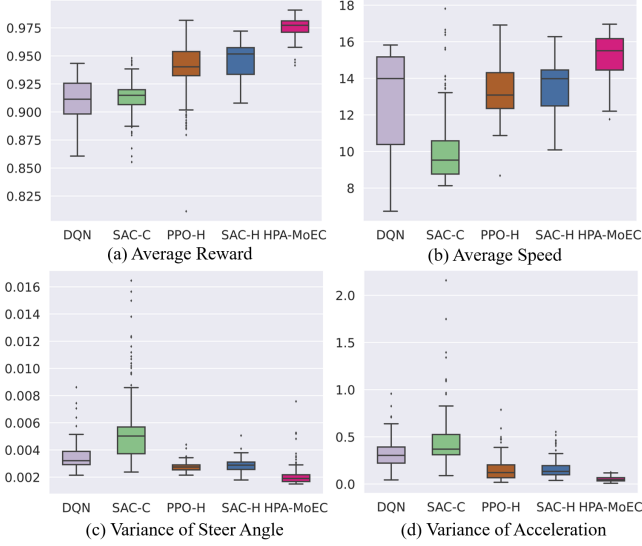


Fig. 5. Metrics distribution of testing in HighD dataset.

TABLE III  
TEST RESULTS IN HIGHD DATASET

Method	AR	AS	NL	VS	VA	CR
DQN	0.909	12.74	8.84	0.0035	0.316	0.29%
SAC-C	0.913	10.12	1.25	0.0054	0.451	0.00%
PPO-H	0.938	13.32	5.67	0.0028	0.155	0.04%
SAC-H	0.945	13.58	5.69	0.0029	0.160	0.05%
HPA-MoEC	0.976	15.27	7.03	0.0021	0.051	0.01%

pared to SAC-H, HPA-MoEC improves AS by 13% and increases NL by 28%. Compared to the above methods with hybrid actions, SAC-C’s direct control of the EV results in the lowest AS and the fewest NL, indicating its inability to effectively leverage lane-changing opportunities to increase speed. Relying on discrete actions, DQN achieves higher AS in some episodes by frequent lane changes, but its overall AS ranks second to last. Overall, the hybrid actions provide greater flexibility and thus improve driving efficiency, especially by using a parameterized action space to generate outputs rather than discretizing part of the continuous actions.

**For action consistency**, HPA-MoEC exhibits the smallest VS and VA, implying a significant reduction in lateral and longitudinal driving behavior fluctuations. In comparison, although PPO-H and SAC-H also generate hybrid actions, their VS increases by 26% and 42%, respectively, while their VA increases by 41% and 54%, respectively. This indicates that the HPA-MoEC generates smoother guiding paths and acceleration commands through its parameterized action space. Notably, both SAC-C and DQN exhibit large VS and VA, indicating large behavior fluctuations. For DQN, the discrete decision set hampers smooth steering adjustments during lane changes and restricts acceleration flexibility. For SAC-C, the coupling between steering angle and acceleration commands makes it extremely challenging to produce smooth and regular outputs when both exhibit fluctuations.

**For safety performance**, HPA-MoEC demonstrates the lowest CR, second only to SAC-C, highlighting its strong

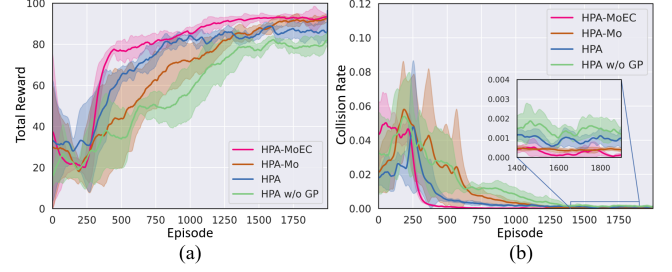


Fig. 6. The training process of our framework with ablation baselines quantified by: a) Total Reward and b) Collision Rate.

focus on safety. This is facilitated by a policy evaluation design with safety attribute as a separate objective, achieving a CR reduction of 67% and 69% for HPA compared to SAC-H and PPO-H, respectively. Notably, SAC-C adopts a highly conservative driving policy, greatly reducing the CR at the cost of driving efficiency. Additionally, DQN has a CR of 0.38%, much higher than other methods. With an average of 7.73 NL per episode, this indicates that its more aggressive driving policy increases the risk of putting the EV in danger.

2) *Testing in HighD-Dataset*: The testing results on the HighD dataset, including the distribution of evaluation metrics and quantitative statistics, are shown in Fig. 5 and Table III, respectively. Compared to the constructed simulation scenario, the traffic density in HighD is sparser, and all methods demonstrate better driving performance. Clearly, HPA-MoEC still achieves the highest AR, showing the good adaptability of its driving policy. It also maintains excellent control over acceleration and flexible lane-changing abilities, resulting in the highest AS and the most NL, except for DQN. Additionally, the guiding path still plays a role in the reduction of vehicle behavior fluctuations, keeping the VS and VA low. In terms of safety, the emphasis on safety attributes in HPA-MoEC reduces the CR to just 0.01%. Overall, HPA-MoEC outperforms all other baselines in terms of compatibility with the objectives of driving efficiency, action consistency, and safety, offering greater potential for real-world traffic applications.

### C. Ablation study

1) *Training Performance*: The changes in total reward and collision rate for all ablation baselines during training are shown in Fig. 6. It is clear that as key components of HPA-MoEC are gradually removed, the performance decreases.

For HPA-Mo, policy convergence is greatly delayed. Compared to HPA-MoEC, HPA-Mo reaches similar final rewards and slightly higher CR. However, its convergence is slower, only reaching around the 1700th episode. In contrast, HPA-MoEC, despite involving more networks, converges around the 1400th episode, suggesting that epistemic uncertainty-based policy exploration improves training efficiency by about 18%.

For HPA, it shows lower rewards and higher CR at convergence compared to HPA-Mo. This suggests that the designed multi-objective compatible policy evaluation architecture is effective. Utilizing critics that specifically target general driving attributes and safety during policy evaluation can promote driving that is compatible with general performance and safety.

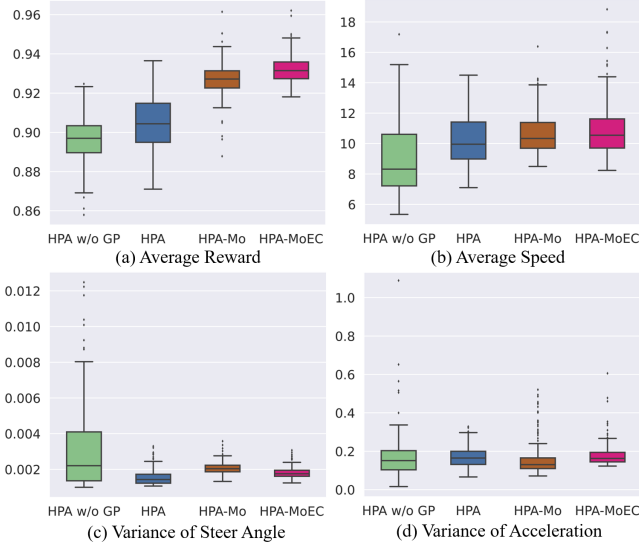


Fig. 7. Metrics distribution of ablation study with rule-based SVs.

TABLE IV  
ABLATIVE STUDIES FOR HPA-MoEC WITH RULE-BASED SVs

Method	AR	AS	NL	VS	VA	CR
HPA-MoEC	0.932	10.87	7.14	0.0019	0.181	0.04%
HPA-Mo	0.927	10.63	6.90	0.0020	0.160	0.03%
HPA	0.905	10.36	6.11	0.0016	0.175	0.08%
HPA w/o GP	0.897	8.92	6.22	0.0032	0.169	0.11%

For HPA w/o GP, there are even lower rewards and higher CR compared to HPAs. This indicates that the introduction of finer-grained guiding paths enhances the connection between the agent’s outputs and driving behavior, leading to further improvements in both general policy performance and safety.

2) *Testing with Rule-Based SVs*: The results of the ablation baseline tests, including data distributions and quantitative statistics, are shown in Fig. 7 and Table IV. The HPA-MoEC, with all technology components, demonstrates the best driving performance. As components are progressively removed, the driving performance of the ablation baselines declines accordingly.

HPA-Mo, although slow in policy convergence during training, shows driving performance close to HPA-MoEC in the final testing, with only a slight reduction in AR and AS.

HPA performs worse in both general driving performance and safety, with lower AR and higher CR. Specifically, removing the multi-objective policy evaluation component leads to a significant decrease in AR and, more importantly, nearly a threefold increase in CR for HPA compared to HPA-Mo. This clearly demonstrates that our design maintains the compatibility of the policy with both general performance and safety during testing.

HPA w/o GP performs the worst across all metrics compared to the other ablation baselines. Notably, removing the guiding path results in approximately a 100% increase in VS compared to HPA, highlighting the larger fluctuations in lateral driving behavior. In addition, its AS decreases by 14%, with a wider distribution, while the CR increases by 38%,

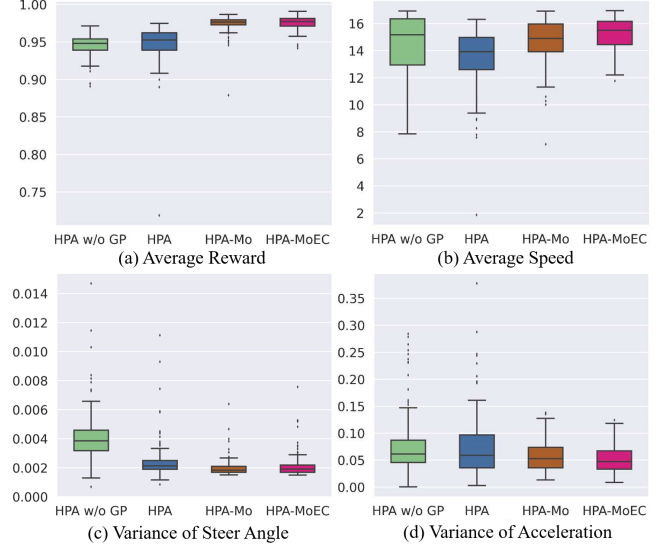


Fig. 8. Metrics distribution of ablation study in HighD dataset.

TABLE V  
ABLATIVE STUDIES FOR HPA-MoEC IN HIGHD DATASET

Method	AR	AS	NL	VS	VA	CR
HPA-MoEC	0.976	15.27	7.03	0.0021	0.051	0.01%
HPA-Mo	0.975	14.71	6.88	0.0019	0.057	0.01%
HPA	0.948	13.49	5.95	0.0024	0.073	0.04%
HPA w/o GP	0.946	14.43	6.08	0.0041	0.077	0.06%

reflecting a decline in both driving efficiency and safety. Therefore, implementing a hybrid parameterized action space with finer-grained guidance paths helps the agent promote multi-objective driving, particularly in terms of reducing fluctuations in driving behavior.

3) *Testing in HighD-Dataset*: The testing results for all ablation baselines in the HighD dataset are shown in Fig. 8 and Table V. HPA-Mo falls slightly below HPA-MoEC in driving efficiency, but both have good driving performance. In contrast, HPA lags clearly behind both previous methods in AS and NL and has a higher CR. The ‘HPA w/o GP’ is even worse, accompanying a notable increase in VS. This suggests that the multi-objective policy evaluation architecture and the hybrid parameterized action space with guiding paths still promote the compatibility of the objectives of driving efficiency, action consistency and safety in the HighD dataset.

#### D. Discussion

In summary, our HPA-MoEC method outperforms all the RL comparison baselines, where all three key technology components play a significant role in facilitating the learning of a multi-objective compatible policy. The hybrid parameterized action enhances the connection between agent actions and driving behavior by simultaneously outputting finer-grained guiding paths as well as direct acceleration commands. This action space structure promotes multi-objective compatibility, particularly enhancing action consistency by reducing driving behavior fluctuations while maintaining flexibility. The multi-objective policy evaluation architecture guides the agent in

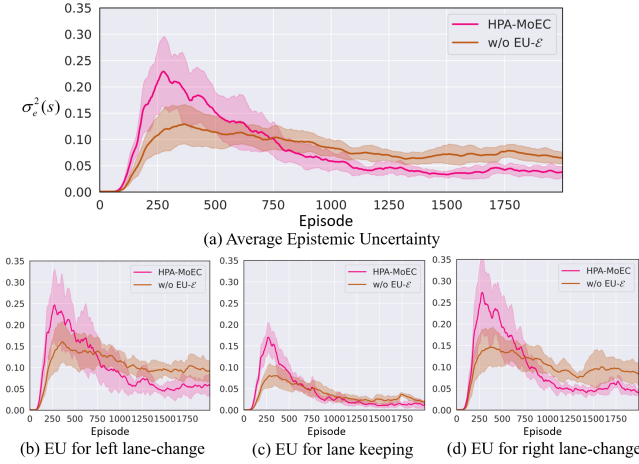


Fig. 9. Changes in epistemic uncertainty (EU) during training, including: a) average epistemic uncertainty, (b) EU for left lane-change, (c) EU for lane keeping, (d) EU for right lane-change.

improving policy learning by treating general and safety attributes as distinct objectives and building the corresponding reward function and critic. This policy evaluation architecture improves both the driving general performance and safety, demonstrating its ability to achieve multi-objective compatible driving. In addition, the epistemic uncertainty-based policy exploration mechanism accelerates the convergence of multi-objective compatible viable policies, improving the training efficiency. Furthermore, the testing in HighD demonstrates that HPA-MoEC remains superior under real scenario datasets and possesses better application prospects.

Additionally, to better observe the impact of our exploration mechanism on epistemic uncertainty, we denote ‘w/o EU- $\epsilon$ ’ as an attempt. In this attempt, ensemble-critics generate epistemic uncertainty but do not use it for exploration, instead performing random exploration. The curves in Figure 1 show how epistemic uncertainty evolves throughout the policy improvement process. Our HPA-MoEC experiences higher average uncertainty in the early training phases, and then makes the uncertainty lower more rapidly during exploration. This suggests that HPA-MoEC explores more fully while converging the policy faster than randomized exploration. Further, the changes in epistemic uncertainty for the three lane-change decisions follow a similar trend. Notably, changing lanes—whether to the left or right—results in higher uncertainty compared to lane keeping, suggesting that lane changes involve greater unknowns and risks.

## VI. CONCLUSION AND FUTURE WORK

This paper proposes a Multi-objective Ensemble-Critic (HPA-MoEC) reinforcement learning method with Hybrid Parameterized Action space, capable of efficiently learning multi-objective compatible driving policies. Our method includes three key components: i) the hybrid parameterized action space that simultaneously generates abstract guidance and concrete control commands, ii) the multi-objective compatible policy evaluation framework that considers multiple driving attributes, and iii) the epistemic uncertainty-based policy ex-

ploration strategy. We conduct the training and testing of the policy in both simulated traffic environments and the HighD dataset. The results show that HPA-MoEC effectively learns a multi-objective compatible autonomous driving policy in terms of efficiency, action consistency, and safety. The ablation study further demonstrated the role of the three technology components in HPA-MoEC in promoting multi-objective compatibility.

Future work aims to further investigate how uncertainty can be leveraged in autonomous driving, particularly to encourage more cautious behavior during testing.

## ACKNOWLEDGMENTS

This work is supported in part by the National Natural Science Foundation of China under Grant No. 52325212 and No.52372394, in part by the National Key R&D Program of China under Grant No. 2022YFE0117100.

## REFERENCES

- [1] A. Y. Majid, S. Saaybi, V. Francois-Lavet, R. V. Prasad, and C. Verhoeven, “Deep reinforcement learning versus evolution strategies: A comparative survey,” *IEEE Trans. Neural Netw. Learn. Sys.*, 2023.
- [2] Y. Zhang, B. Gao, L. Guo, H. Guo, and H. Chen, “Adaptive decision-making for automated vehicles under roundabout scenarios using optimization embedded reinforcement learning,” *IEEE Trans. Neural Netw. Learn. Sys.*, vol. 32, no. 12, pp. 5526–5538, 2021.
- [3] J. Hao, T. Yang, H. Tang, C. Bai, J. Liu, Z. Meng, P. Liu, and Z. Wang, “Exploration in deep reinforcement learning: From single-agent to multiagent domain,” *IEEE Trans. Neural Netw. Learn. Sys.*, vol. 35, no. 7, pp. 8762–8782, 2024.
- [4] Z. He, L. Dong, C. Song, and C. Sun, “Multiagent soft actor-critic based hybrid motion planner for mobile robots,” *IEEE Trans. Neural Netw. Learn. Sys.*, vol. 34, no. 12, pp. 10980–10992, 2022.
- [5] J. Xing, D. Wei, S. Zhou, T. Wang, Y. Huang, and H. Chen, “A comprehensive study on self-learning methods and implications to autonomous driving,” *IEEE Trans. Neural Netw. Learn. Sys.*, pp. 1–20, 2024.
- [6] Z. Li, G. Jin, R. Yu, B. Leng, and L. Xiong, “Interaction-aware deep reinforcement learning approach based on hybrid parameterized action space for autonomous driving,” in *Proc. SAE Intell. Connected Veh. Symposium (SAE ICVS)*, 2024.
- [7] P. R. Wurman, S. Barrett, K. Kawamoto, J. MacGlashan, K. Subramanian, T. J. Walsh, R. Capobianco, A. Devlic, F. Eckert, F. Fuchs, *et al.*, “Outracing champion gran turismo drivers with deep reinforcement learning,” *Nature*, vol. 602, no. 7896, pp. 223–228, 2022.
- [8] W. B. Knox, A. Allievi, H. Banzhaf, F. Schmitt, and P. Stone, “Reward (mis) design for autonomous driving,” *Artif. Intell.*, vol. 316, p. 103829, 2023.
- [9] Z. Zhu and H. Zhao, “A survey of deep rl and il for autonomous driving policy learning,” *IEEE Trans. Intell. Transp. Syst.*, vol. 23, no. 9, pp. 14043–14065, 2022.
- [10] G. Li, Y. Qiu, Y. Yang, Z. Li, S. Li, W. Chu, P. Green, and S. E. Li, “Lane change strategies for autonomous vehicles: A deep reinforcement learning approach based on transformer,” *IEEE Trans. Intell. Veh.*, vol. 8, no. 3, pp. 2197–2211, 2023.
- [11] X. Lu, F. X. Fan, and T. Wang, “Action and trajectory planning for urban autonomous driving with hierarchical reinforcement learning,” *arXiv preprint arXiv:2306.15968*, 2023.
- [12] L. Chen, Y. He, Q. Wang, W. Pan, and Z. Ming, “Joint optimization of sensing, decision-making and motion-controlling for autonomous vehicles: A deep reinforcement learning approach,” *IEEE Trans. Veh. Technol.*, vol. 71, no. 5, pp. 4642–4654, 2022.
- [13] P. Ladosz, L. Weng, M. Kim, and H. Oh, “Exploration in deep reinforcement learning: A survey,” *Inf. Fusion*, vol. 85, pp. 1–22, 2022.
- [14] X. Wang, S. Wang, X. Liang, D. Zhao, J. Huang, X. Xu, B. Dai, and Q. Miao, “Deep reinforcement learning: A survey,” *IEEE Trans. Neural Netw. Learn. Sys.*, vol. 35, no. 4, pp. 5064–5078, 2024.
- [15] S. Nagesh Rao, H. E. Tseng, and D. Filev, “Autonomous highway driving using deep reinforcement learning,” in *Proc. IEEE Int. Conf. Syst. Man Cybern. (SMC)*, pp. 2326–2331, 2019.

- [16] S. Li, C. Wei, and Y. Wang, "Combining decision making and trajectory planning for lane changing using deep reinforcement learning," *IEEE Trans. Intell. Transp. Syst.*, vol. 23, no. 9, pp. 16110–16136, 2022.
- [17] P. Wolf, K. Kurzer, T. Wingert, F. Kuhnt, and J. M. Zollner, "Adaptive behavior generation for autonomous driving using deep reinforcement learning with compact semantic states," in *Proc. IEEE Intell. Veh. Symposium (IV)*, pp. 993–1000, 2018.
- [18] G. Chen, Y. Zhang, and X. Li, "Attention-based highway safety planner for autonomous driving via deep reinforcement learning," *IEEE Trans. Veh. Technol.*, 2023.
- [19] Y. Yu, C. Lu, L. Yang, Z. Li, F. Hu, and J. Gong, "Hierarchical reinforcement learning combined with motion primitives for automated overtaking," in *Proc. IEEE Intell. Veh. Symposium (IV)*, pp. 1–6, 2020.
- [20] G. Jin, Z. Li, B. Leng, and M. Shao, "Deep reinforcement learning lane-change decision-making for autonomous vehicles based on motion primitives library in hierarchical action space," *Artificial Intelligence and Autonomous Systems*, vol. 2, no. 0009, 2024.
- [21] X. Lu, F. X. Fan, and T. Wang, "Action and trajectory planning for urban autonomous driving with hierarchical reinforcement learning," *arXiv:2306.15968*, 2023.
- [22] Z. Wang, H. Huang, J. Tang, and L. Hu, "A deep reinforcement learning-based approach for autonomous lane-changing velocity control in mixed flow of vehicle group level," *Expert Syst. Appl.*, vol. 238, p. 122158, 2024.
- [23] Z. Qi, T. Wang, J. Chen, D. Narang, Y. Wang, and H. Yang, "Learning-based path planning and predictive control for autonomous vehicles with low-cost positioning," *IEEE Trans. Intell. Veh.*, vol. 8, no. 2, pp. 1093–1104, 2023.
- [24] Anonymous, "Flipnet: Fourier lipschitz smooth policy network for reinforcement learning," in *Submitted to The 30th Proc. Int. Conf. Learn. Representations (ICLR)*, 2024, under review.
- [25] Q. Guo, O. Angah, Z. Liu, and X. J. Ban, "Hybrid deep reinforcement learning based eco-driving for low-level connected and automated vehicles along signalized corridors," *Transp. Res. Part C Emerg. Technol.*, vol. 124, p. 102980, 2021.
- [26] Z. Wei, P. Hao, and M. J. Barth, "Developing an adaptive strategy for connected eco-driving under uncertain traffic condition," in *Proc. IEEE Intell. Veh. Symposium (IV)*, pp. 2066–2071, 2019.
- [27] H. Liu, Z. Huang, X. Mo, and C. Lv, "Augmenting reinforcement learning with transformer-based scene representation learning for decision-making of autonomous driving," *IEEE Trans. Intell. Veh.*, vol. 9, no. 3, pp. 4405–4421, 2024.
- [28] Y. Lin, X. Liu, and Z. Zheng, "Discretionary lane-change decision and control via parameterized soft actor-critic for hybrid action space," *Machines*, vol. 12, no. 4, p. 213, 2024.
- [29] J. Peng, S. Zhang, Y. Zhou, and Z. Li, "An integrated model for autonomous speed and lane change decision-making based on deep reinforcement learning," *IEEE Trans. Intell. Transp. Syst.*, vol. 23, no. 11, pp. 21848–21860, 2022.
- [30] Y. Gurses, K. Buyukdemirci, and Y. Yildiz, "Developing driving strategies efficiently: A skill-based hierarchical reinforcement learning approach," *IEEE Control Syst. Lett.*, 2024.
- [31] G. Jin, Z. Li, B. Leng, W. Han, and L. Xiong, "Stability enhanced hierarchical reinforcement learning for autonomous driving with parameterized trajectory action," in *Proc. IEEE Intell. Transp. Syst. Conf. (ITSC)*, 2024.
- [32] A. Abouelazm, J. Michel, and J. M. Zoellner, "A review of reward functions for reinforcement learning in the context of autonomous driving," *arXiv preprint arXiv:2405.01440*, 2024.
- [33] X. Wen, S. Jian, and D. He, "Modeling the effects of autonomous vehicles on human driver car-following behaviors using inverse reinforcement learning," *IEEE Trans. Intell. Transp. Syst.*, 2023.
- [34] D. Amodi, C. Olah, J. Steinhardt, P. Christiano, J. Schulman, and D. Mané, "Concrete problems in ai safety," *arXiv preprint arXiv:1606.06565*, 2016.
- [35] S. Mysore, G. Cheng, Y. Zhao, K. Saenko, and M. Wu, "Multi-critic actor learning: Teaching rl policies to act with style," in *Proc. Int. Conf. Learn. Representations (ICLR)*, 2022.
- [36] Z. Wang, S. Zhang, X. Feng, and Y. Sui, "Autonomous underwater vehicle path planning based on actor-multi-critic reinforcement learning," *Proceedings of the Institution of Mechanical Engineers, Part I: Journal of Systems and Control Engineering*, vol. 235, no. 10, pp. 1787–1796, 2021.
- [37] K. Yang, X. Tang, S. Qiu, S. Jin, Z. Wei, and H. Wang, "Towards robust decision-making for autonomous driving on highway," *IEEE Trans. Veh. Technol.*, vol. 72, no. 9, pp. 11251–11263, 2023.
- [38] X. He and C. Lv, "Toward personalized decision making for autonomous vehicles: a constrained multi-objective reinforcement learning technique," *Transp. Res. Part C Emerg. Technol.*, vol. 156, p. 104352, 2023.
- [39] K. Srinivasan, B. Eysenbach, S. Ha, J. Tan, and C. Finn, "Learning to be safe: Deep rl with a safety critic," *arXiv preprint arXiv:2010.14603*, 2020.
- [40] Q. Liu, Y. Li, S. Chen, K. Lin, X. Shi, and Y. Lou, "Distributional reinforcement learning with epistemic and aleatoric uncertainty estimation," *Inf. Sci.*, vol. 644, p. 119217, 2023.
- [41] M. Tokic, "Adaptive  $\epsilon$ -greedy exploration in reinforcement learning based on value differences," in *KI 2010: Advances in Artif. Intell.*, pp. 203–210, Springer, 2010.
- [42] R. Chai, H. Niu, J. Carrasco, F. Arvin, H. Yin, and B. Lennox, "Design and experimental validation of deep reinforcement learning-based fast trajectory planning and control for mobile robot in unknown environment," *IEEE Trans. Neural Netw. Learn. Sys.*, vol. 35, no. 4, pp. 5778–5792, 2022.
- [43] M. C. Machado, M. G. Bellemare, and M. Bowling, "Count-based exploration with the successor representation," vol. 34, no. 04, pp. 5125–5133, 2020.
- [44] M. Usama and D. E. Chang, "Learning-driven exploration for reinforcement learning," in *Int. Conf. Control, Autom. Syst. (ICCAS)*, pp. 1146–1151, IEEE, 2021.
- [45] J. Wu, Z. Huang, W. Huang, and C. Lv, "Prioritized experience-based reinforcement learning with human guidance for autonomous driving," *IEEE Trans. Neural Netw. Learn. Sys.*, vol. 35, no. 1, pp. 855–869, 2024.
- [46] J. Zhang, B. Cheung, C. Finn, S. Levine, and D. Jayaraman, "Cautious adaptation for reinforcement learning in safety-critical settings," in *Int. Conf. Mach. Learn. (ICML)*, pp. 11055–11065, PMLR, 2020.
- [47] D. Kim, J. Shin, P. Abbeel, and Y. Seo, "Accelerating reinforcement learning with value-conditional state entropy exploration," *Adv. Neural Inf. Process. Syst. (NeurIPS)*, vol. 36, 2024.
- [48] Z. Zhang, Q. Liu, Y. Li, K. Lin, and L. Li, "Safe reinforcement learning in autonomous driving with epistemic uncertainty estimation," *IEEE Trans. Intell. Transp. Syst.*, 2024.
- [49] V. S. Borkar, "Stochastic approximation with two time scales," *Systems & Control Letters*, vol. 29, no. 5, pp. 291–294, 1997.
- [50] C.-J. Hoel, K. Wolff, and L. Laine, "Tactical decision-making in autonomous driving by reinforcement learning with uncertainty estimation," in *Proc. IEEE Intell. Veh. Symposium (IV)*, pp. 1563–1569, 2020.
- [51] E. Leurent, "An environment for autonomous driving decision-making," <https://github.com/eleurent/highway-env>, 2018.
- [52] R. Krajewski, J. Bock, L. Kloecker, and L. Eckstein, "The highd dataset: A drone dataset of naturalistic vehicle trajectories on german highways for validation of highly automated driving systems," in *Proc. IEEE Intell. Transp. Syst. Conf. (ITSC)*, pp. 2118–2125, 2018.
- [53] V. Mnih, K. Kavukcuoglu, D. Silver, A. A. Rusu, J. Veness, M. G. Bellemare, A. Graves, M. Riedmiller, A. K. Fidjeland, G. Ostrovski, et al., "Human-level control through deep reinforcement learning," *nature*, vol. 518, no. 7540, pp. 529–533, 2015.
- [54] T. Haarnoja, A. Zhou, P. Abbeel, and S. Levine, "Soft actor-critic: Off-policy maximum entropy deep reinforcement learning with a stochastic actor," in *Int. Conf. Mach. Learn. (ICML)*, pp. 1861–1870, PMLR, 2018.
- [55] J. Schulman, "Trust region policy optimization," *arXiv preprint arXiv:1502.05477*, 2015.